



Infrared Spectroscopy of Molecular Submonolayers on Surfaces by Infrared Scanning Tunneling Microscopy: Tetramantane on Au(111)

Ivan V. Pechenezhskiy,^{1,2} Xiaoping Hong,¹ Giang D. Nguyen,¹ Jeremy E. P. Dahl,³
 Robert M. K. Carlson,³ Feng Wang,¹ and Michael F. Crommie^{1,2,*}

¹*Department of Physics, University of California at Berkeley, Berkeley, California 94720, USA*

²*Materials Sciences Division, Lawrence Berkeley National Laboratory, Berkeley, California 94720, USA*

³*Stanford Institute for Materials and Energy Science, Stanford University, Stanford, California 94305, USA*

(Received 1 May 2013; published 16 September 2013)

We have developed a new scanning-tunneling-microscopy-based spectroscopy technique to characterize infrared (IR) absorption of submonolayers of molecules on conducting crystals. The technique employs a scanning tunneling microscope as a precise detector to measure the expansion of a molecule-decorated crystal that is irradiated by IR light from a tunable laser source. Using this technique, we obtain the IR absorption spectra of [121]tetramantane and [123]tetramantane on Au(111). Significant differences between the IR spectra for these two isomers show the power of this new technique to differentiate chemical structures even when single-molecule-resolved scanning tunneling microscopy (STM) images look quite similar. Furthermore, the new technique was found to yield significantly better spectral resolution than STM-based inelastic electron tunneling spectroscopy, and to allow determination of optical absorption cross sections. Compared to IR spectroscopy of bulk tetramantane powders, infrared scanning tunneling microscopy (IRSTM) spectra reveal narrower and blueshifted vibrational peaks for an ordered tetramantane adlayer. Differences between bulk and surface tetramantane vibrational spectra are explained via molecule-molecule interactions.

DOI: [10.1103/PhysRevLett.111.126101](https://doi.org/10.1103/PhysRevLett.111.126101)

PACS numbers: 68.43.Pq, 33.20.Ea, 63.22.Kn, 68.37.Ef

Simultaneously probing the vibrational behavior and local electronic or geometric structure of molecular adsorbates is important for understanding their physical and chemical properties. Scanning tunneling microscopy (STM) is a powerful tool for this purpose since it can yield subnanometer-resolved topographical information and orbital energetics, as well as vibrational properties through inelastic electron tunneling spectroscopy (STM IETS) [1,2]. Electron-based STM IETS, however, does not allow direct probing of optical processes and has a spectral resolution limited by thermal broadening. STM-induced luminescence [3–7] and tip-enhanced Raman spectroscopy [8–10] are related techniques that do give simultaneous local and optovibrational information. STM-induced luminescence, however, can so far probe only selected vibrational modes through vibronic transitions and has energy resolution that is partially limited by electronic excited state lifetimes, while tip-enhanced Raman spectroscopy is limited to dye-like molecules with large Raman cross sections and usually requires satisfying the resonant Raman condition [11]. Atomic force microscopy infrared spectroscopy (photothermal induced resonance) [12–15] is an additional technique that has been employed to acquire local infrared (IR) absorption spectra and images of surface structures, but this technique works only for high-coverage aggregates of thickness >40–80 nm [14,15] and so cannot yet address the adsorbate-dominated submonolayer regime.

Here, we demonstrate a new STM-based vibrational spectroscopy which overcomes many of the drawbacks of

the above-mentioned techniques by using the STM as a sensitive detector to probe the IR response of adsorbed molecular assemblies. Although our technique is not yet capable of performing single-molecule-resolved IR spectroscopy (it averages over a wider surface area), the technique can be used to probe a wide range of molecular species at submonolayer coverages and with the subthermal energy resolution inherent to IR spectroscopy, while the surface can be simultaneously characterized by conventional STM imaging. We refer to this new technique as infrared scanning tunneling microscopy (IRSTM). Using IRSTM, we have obtained IR absorption spectra and STM images of submonolayer coverages of the diamondoid molecules [121]tetramantane and [123]tetramantane deposited onto Au(111). Significant differences in IRSTM spectra for these two isomers demonstrate the power of IRSTM to differentiate individual chemical species and to determine molecular vibrational properties in different surface environments. Our analysis of tetramantane IRSTM spectra allows us to conclude that tetramantane vibrational resonances are more strongly affected by intermolecular interactions than by interactions between the tetramantane molecules and the gold surface.

The main idea of IRSTM is to employ an STM tip in tunneling mode to detect the thermal expansion of a sample due to the molecular absorption of tunable, monochromatic IR radiation. When a bare crystal is irradiated, thermal expansion of the crystal in the direction perpendicular to its surface can be measured by monitoring the motion of an

STM tip in constant-current mode. When the surface is covered by adsorbed molecules, however, a new absorption channel appears whenever the wavelength of light is tuned to a molecular vibrational resonance. Excited vibrational states of a molecule typically relax in ~ 10 ps [16], and the associated energy is transferred to the substrate. Therefore, the extra expansion (the difference between the surface expansion with and without molecules) at a given wavelength yields the molecular absorption at this wavelength.

IRSTM was used to measure IR absorption spectra of tetramantane molecules at coverages of less than one monolayer on a Au(111) surface. [121]tetramantane [inset of Fig. 1(a)] and [123]tetramantane [inset of Fig. 1(b)] were chosen because they are structural isomers described by the same chemical formula $C_{22}H_{28}$, and also because [121]tetramantane on Au(111) exhibits a pronounced CH stretch mode that has been previously observed using STM IETS [17]. The molecules were extracted from petroleum and purified into powder form [18]. The powders were sublimated in vacuum at temperatures in the range of 30°C – 34°C onto a clean Au(111) surface held at room temperature, resulting in coverages ranging from 0.5 to 1.0 monolayer (ML). STM measurements were performed using a homemade ultrahigh vacuum (UHV) variable temperature STM operating at $T = 13$ – 15 K. Figures 1(a) and 1(b) show typical STM images of [121]tetramantane/Au(111) and [123]tetramantane/Au(111), respectively. The two molecules look similar in their topography, although the [121]tetramantane packaging is slightly elongated in the direction of the molecular lattice vector labeled **a** [Fig. 1(a)].

IR excitation of the tetramantane/Au(111) surface was performed using a homemade tunable mode-hop-free laser. The main components of the tunable IR laser are

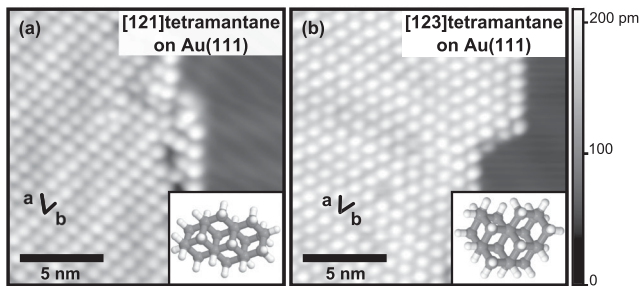


FIG. 1. (a) STM topography of [121]tetramantane molecules on Au(111) ($V_{\text{sample}} = 1.0$ V, $I = 50$ pA, $T = 13$ K). The molecular lattice has an oblique structure with lattice constants $|\mathbf{a}| = 11.1 \pm 0.1$ Å, $|\mathbf{b}| = 8.3 \pm 0.1$ Å, and an interior angle of $59^\circ \pm 1^\circ$. The inset shows a model of [121]tetramantane (gray and white balls represent carbon and hydrogen atoms). (b) STM topography of [123]tetramantane on a Au(111) surface ($V_{\text{sample}} = -2.0$ V, $I = 100$ pA, $T = 13$ K). Within experimental resolution, [123]tetramantane molecules form a hexagonal structure with $|\mathbf{a}| = |\mathbf{b}| = 9.8 \pm 0.1$ Å. The inset shows a model of *P* [123]tetramantane [our [123]tetramantane/Au(111) samples were prepared from a racemic mixture containing *P* and *M* enantiomers].

schematically shown in Fig. 2. A singly resonant optical parametric oscillator (OPO) based on periodically poled MgO-doped lithium niobate was employed to down-convert the light frequency from a pump laser. The pump laser consists of an external cavity laser diode as a seed laser light source and an optical amplifier. Pump tuning with synchronous periodically poled MgO-doped lithium niobate temperature control was used to deliver continuous frequency tuning of the IR OPO output, as reported elsewhere [19]. A feedback loop was used to stabilize the IR light intensity at the OPO output to suppress fluctuations down to about 0.5% of the overall intensity. The laser beam (total power ~ 30 mW) was guided into the UHV STM chamber through a CaF_2 viewport. The beam was converged via an external lens to achieve a spot size of 1.2 mm diameter on the sample. The beam center was intentionally targeted to a point on the surface 0.8–1.5 mm away from the STM junction. This was done to avoid direct light excitation of the tip-sample tunnel junction, thus eliminating the effects of tip thermal expansion, rectification, and thermoelectric current generation [20]. Under these conditions, no significant difference, apart from overall amplitude variation, was found between IRSTM spectra taken at different lateral distances between the laser spot and the tunnel junction, or with different laser spot sizes.

IRSTM spectra were measured via two different modes: with optical chopping of the laser light (ac mode) and without optical chopping (dc mode). Figure 3(a) shows the IRSTM spectrum of a single monolayer of [121]tetramantane measured using the ac mode. Here, the differential STM *Z* signal was measured under constant-current feedback conditions (via lock-in detection at the chopping frequency) while sweeping the IR excitation from 2830 to 2940 cm^{-1} . The same measurement was performed on bare Au(111) as a reference. Six IR absorption peaks can clearly be seen for [121]tetramantane/Au(111) compared to the bare Au(111) spectrum at 2850 ± 1 , 2855 ± 1 , 2881 ± 1 , 2897 ± 1 , 2909 ± 1 , and 2920 ± 1 cm^{-1} . The appearance of these peaks indicates a larger thermal expansion

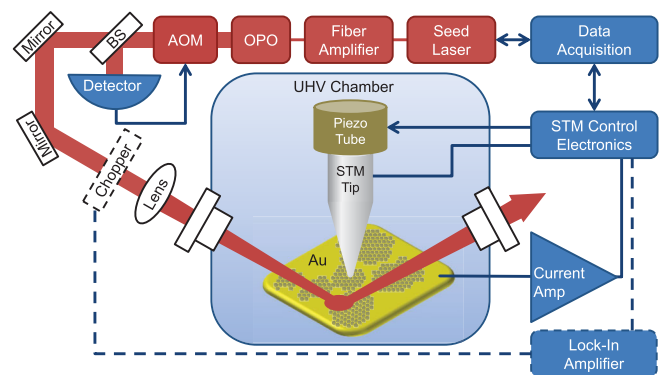


FIG. 2 (color). Experimental setup combining a tunable IR laser and a UHV STM. The IR light intensity is stabilized by a feedback loop consisting of an acousto-optic modulator (AOM), a beam splitter (BS), and a diode detector. The IR light was directed into the STM as described in the text. A lock-in amplifier and chopper were used for ac measurements.

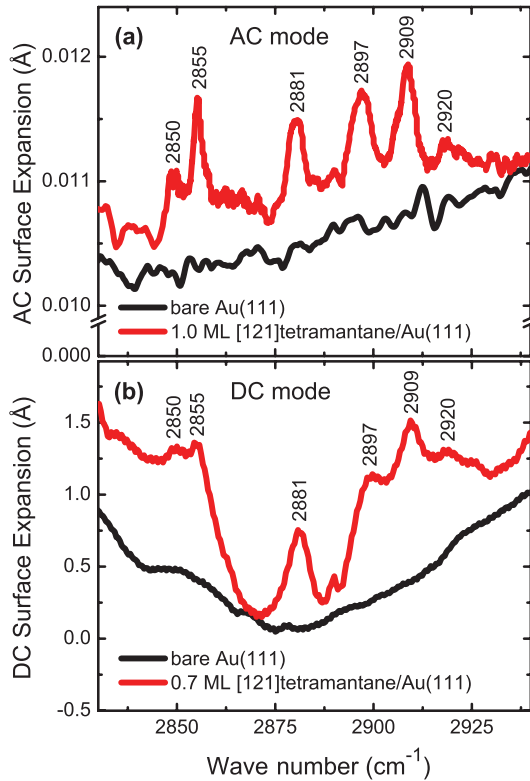


FIG. 3 (color). (a) Differential ac surface expansion due to absorption of modulated IR light, measured via lock-in amplifier for constant-current STM Z signal (chopper modulation frequency ~ 13 Hz, lock-in amplifier time constant 3 s). The black (lower) and red (upper) lines show ac surface expansion of bare gold and [121]tetramantane-decorated gold, respectively. (b) dc surface expansion of bare gold (black lower line) and [121]tetramantane-decorated gold (red upper line) as a function of incident IR frequency, measured via constant-current STM Z signal.

amplitude at the corresponding IR frequencies and, therefore, can be attributed to extra energy absorption by [121]tetramantane vibrational modes at these frequencies. The ratio of the peak heights [$\sim 7 \times 10^{-4}$ Å for the major peaks shown in Fig. 3(a)] to the background level [$\sim 1 \times 10^{-2}$ Å in Fig. 3(a)] corresponds to the relative absorption of the [121]tetramantane monolayer compared to the bare gold absorption. Assuming that polished gold at low temperatures absorbs $\sim 1\%$ of incoming IR light [21,22], the ratio of the major peak height to the background level yields a molecular absorption coefficient of $\sim 0.07\%$ for one monolayer of [121]tetramantane. This corresponds to an absorption cross section of $\sim 6 \times 10^{-18}$ cm² per molecule.

We also performed IRSTM measurements of [121]tetramantane using the dc mode (a measurement with no optical chopping). This is a simpler measurement than the ac mode, since the ac mode requires low optical chopping frequencies and long lock-in time constants. Figure 3(b) shows the dc IRSTM spectrum of 0.7 ML of [121]tetramantane on Au(111), as well as a bare Au(111) reference spectrum. The [121]tetramantane/Au(111) spectrum shows

peaks relative to the bare Au(111) spectrum at the same energy positions as in Fig. 3(a). These peaks are therefore attributed to extra light absorption by [121]tetramantane molecules. The dc IRSTM spectra reflect the same information as ac spectra, but the peak amplitude is harder to quantitatively interpret due to the lack of a well-defined overall absorption reference point (i.e., such as the bare gold absorption). The dc spectra are also more strongly affected by unavoidable drifts in the experimental setup. These drifts are caused by redistribution of the thermal fluxes inside the STM due to the fact that the tip-sample temperature equilibrium depends very sensitively on parameters such as sample orientation, beam path, and laser power stability. We note, however, that after a baseline subtraction [i.e., subtraction of a third order polynomial fit to the estimated bare Au(111) contribution to the spectrum], the vibrational spectra look very similar for both ac and dc measurement modes.

In order to demonstrate the potential of IRSTM for chemical characterization, IRSTM spectroscopy was additionally performed on samples of [123]tetramantane. As seen in Fig. 1, both molecular species form similar self-assembled overlayer structures on Au(111). Figure 4 shows dc IRSTM spectra of 1 ML of [121]tetramantane on Au(111) versus 0.9 ML of [123]tetramantane on Au(111) (after baseline subtraction). The two spectra are clearly distinct from each other, and both exhibit several well-resolved peaks. Peak energies were extracted by fitting Lorentzian lines to the spectra (fits can be seen in Fig. 4). [123]tetramantane/Au(111) vibrational peaks are found at 2852 ± 1 , 2866 ± 1 , 2876 ± 1 , 2908 ± 1 , and 2915 ± 1 cm⁻¹, while the [121]tetramantane/Au(111) peaks are seen at 2850 ± 1 , 2855 ± 1 , 2881 ± 1 , 2897 ± 1 , 2909 ± 1 , and 2920 ± 1 cm⁻¹. This illustrates the power of IRSTM to distinguish submonolayer amounts of even closely related chemical compounds.

It is instructive to discuss some differences between IRSTM spectroscopy and STM IETS. Figure 4(a) shows a d^2I/dV^2 spectrum of [121]tetramantane/Au(111) from Ref. [17] (the blue line having only one broad peak). The IETS peak (obtained at the lower temperature of $T = 7$ K with bias modulation voltage amplitude $V_m = 1\text{--}10$ mV) is much broader in energy and cannot resolve any of the multiple CH stretch modes that exist in this energy range. Since IETS energy resolution depends on temperature and bias modulation voltage amplitude [23], the IETS spectral resolution in Ref. [17] is estimated to be 30 cm⁻¹ at best. In contrast, the energy resolution for IRSTM is determined by the spectral accuracy of the laser. For tunable IR lasers, the spectral uncertainty mainly arises from mode hops which cause sudden changes in the frequency of emitted light. The laser used here was found to be nearly free of mode hopping over the scanned frequency range from 2830 to 2940 cm⁻¹ (an average of three hops occurs per scan, each of magnitude < 1 cm⁻¹) [19]. We therefore conservatively estimate the spectral resolution of IRSTM to be no worse than 1 cm⁻¹ across the frequency range explored here. It should be noted that IRSTM also differs from

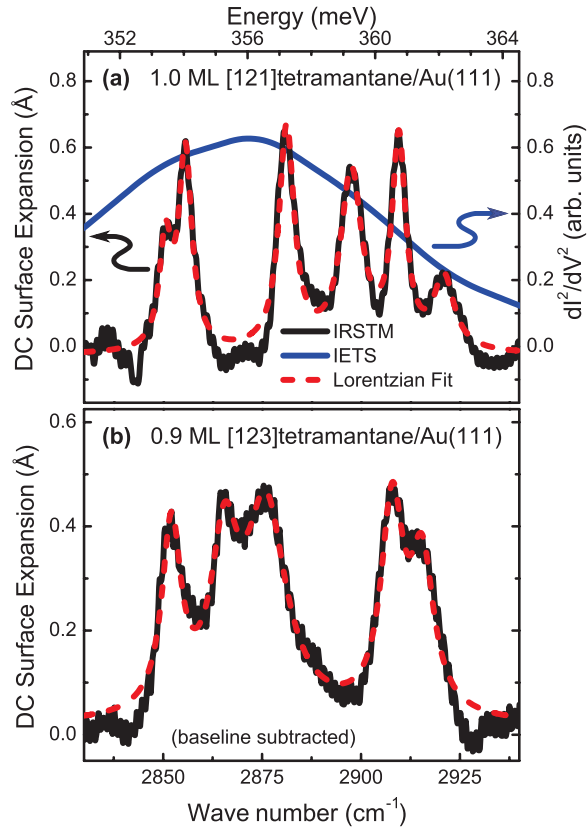


FIG. 4 (color). dc surface expansion due to molecular IR absorption as a function of incident IR frequency. (a) The black solid line shows the average dc surface expansion of [121] tetramantane/Au(111) (five sweeps) with gold baseline signal subtracted. The blue line (with a single broad peak) shows an STM d^2I/dV^2 spectrum of [121]tetramantane/Au(111) from Ref. [17]. (b) The black solid line shows the average dc surface expansion of [123]tetramantane/Au(111) (twelve sweeps) with gold baseline signal subtracted. The red dashed lines are (a) six-peak and (b) five-peak Lorentzian fits to the experimental data.

STM IETS in that IRSTM probes IR active vibrational modes with the dipole moment perpendicular to the metal surface, while STM IETS active modes do not obey rigorous selection rules [24,25].

The linewidths observed using IRSTM carry information regarding molecular interactions. Our tetramantane/Au(111) linewidths were found to be in the range of $4\text{--}12\text{ cm}^{-1}$ (full width at half maximum), corresponding to vibrational lifetimes in the range of $0.4\text{--}1.3\text{ ps}$. Our experimental energy resolution ($\leq 1\text{ cm}^{-1}$) and the homogeneity of our samples imply that this broadening is not instrumental but is rather due to molecule-molecule and molecule-substrate interactions (as well as possibly overlapping modes). We observed notably less broadening of tetramantane CH stretch modes for molecules on Au(111) compared to previously measured powder samples (typical widths for the powder measurements [26] are on the order of $10\text{--}20\text{ cm}^{-1}$). Two main factors likely account for this difference: measurement temperature ($13\text{--}15\text{ K}$ for the surface measurements versus room temperature for the

powder measurements) and structural differences between surface and bulk systems. Regarding structure, our surface measurements were performed on well-ordered adlayers, while the spectra reported in Ref. [26] were obtained on powders lacking perfect crystalline order. Inhomogeneous broadening of the vibrational peaks in the powders is thus expected to be larger than in monolayers on Au(111). Other aspects of the local environment, such as the number of nearest neighbors and the relative coupling strengths between them, can also affect peak broadening. Molecules arranged in two-dimensional lattices (as measured here) are surrounded by a smaller number of nearest neighbors and so can be expected to exhibit smaller broadening compared to the three-dimensional environment experienced by molecules in a powder. Interaction of molecules with a metal substrate, on the other hand, is expected to broaden peaks. Since we see an overall narrowing of vibrational peak widths compared to bulk measurements, we conclude that the narrowing effects of lower temperature and reduction in coordination dominate over the broadening effects of the molecule-surface interaction.

Further information regarding molecule-molecule interactions can be inferred by comparing IRSTM measurements to bulk measurements performed on powder samples. Peaks at notably different energies are observed in bulk powders of different tetramantane isomers, specifically at $2840, 2863, 2884,$ and 2901 cm^{-1} for [121]tetramantane and at $2847, 2871,$ and 2903 cm^{-1} for [123]tetramantane [26]. There is not a perfect one-to-one correspondence between these bulk vibrational modes and the adsorbate modes reported here, but the peaks for the surface measurements do appear overall to be shifted to higher frequencies. We assume this is not due to mechanical renormalization [27] since the molecules are not strongly bonded to the metal surface [17]. Furthermore, neither chemical nor electrostatic shifts are expected to be significant since tetramantane molecules have a large gap between the highest occupied and lowest unoccupied molecular levels, and therefore very little charge transfer between molecules and the gold surface is expected to occur [17]. Two mechanisms that might be at work here are the coupling of dynamic molecular dipole moments to substrate image charges (a redshifting effect) and dynamic dipole-dipole coupling between molecules (a blueshifting effect) [27]. The fact that the vibrational peaks for surface-adsorbed molecules tend to be blueshifted relative to the peaks for powder samples implies that intermolecular dipole-dipole coupling for the surface samples plays a more important role than coupling of the dynamic dipole moments to their images in the substrate. This is consistent with recent observations of appreciable attractive van der Waals interactions in diamondoid dimer structures [28,29].

In conclusion, we have demonstrated the feasibility of IRSTM for performing IR spectroscopic studies of molecular submonolayers on metallic surfaces by combining a tunable IR laser and an STM. We have shown that the excellent spectral resolution of IRSTM can be used for

chemical characterization of molecular adlayers, as well as for measurements of single-molecule optical absorption cross sections. IRSTM measurements of tetramantane molecules on gold reveal that adsorbed tetramantane vibrational peaks are narrowed and blueshifted relative to bulk measurements, implying that intermolecular interactions for adsorbed tetramantane have a stronger influence on molecular vibrational resonances than the interaction between tetramantane molecules and the gold surface. Regarding the ultimate sensitivity of this new technique, we believe that lasers with better intensity stabilization and substrates with an increased thermal expansion coefficient (such as based on a bimetallic strip principle) could significantly improve the IRSTM sensitivity compared to the sensitivity achieved in this work.

This research was supported by the Director, Office of Science, Office of Basic Energy Sciences, Materials Sciences and Engineering Division, U.S. Department of Energy under Contract No. DE-AC03-76SF0098 (STM measurements) and Contract No. DE-AC02-76SF00515 (tetramantane isolation), and by the Department of Energy Early Career Award DE-SC0003949 (development of the IR laser source). I. V. P., X. H., and G. D. N. contributed equally to this work.

*crommie@berkeley.edu

- [1] B. C. Stipe, M. A. Rezaei, and W. Ho, *Science* **280**, 1732 (1998).
- [2] N. Lorente, M. Persson, L. J. Lauhon, and W. Ho, *Phys. Rev. Lett.* **86**, 2593 (2001).
- [3] R. Berndt, R. Gaisch, J. K. Gimzewski, B. Reihl, R. R. Schlittler, W. D. Schneider, and M. Tschudy, *Science* **262**, 1425 (1993).
- [4] X. H. Qiu, G. V. Nazin, and W. Ho, *Science* **299**, 542 (2003).
- [5] Z.-C. Dong, X.-L. Guo, A. S. Trifonov, P. S. Dorozhkin, K. Miki, K. Kimura, S. Yokoyama, and S. Mashiko, *Phys. Rev. Lett.* **92**, 086801 (2004).
- [6] Z. C. Dong, X. L. Zhang, H. Y. Gao, Y. Luo, C. Zhang, L. G. Chen, R. Zhang, X. Tao, Y. Zhang, J. L. Yang, and J. G. Hou, *Nat. Photonics* **4**, 50 (2010).
- [7] C. Chen, P. Chu, C. A. Bobisch, D. L. Mills, and W. Ho, *Phys. Rev. Lett.* **105**, 217402 (2010).
- [8] A. Hartschuh, *Angew. Chem., Int. Ed. Engl.* **47**, 8178 (2008).
- [9] J. Steidtner and B. Pettinger, *Phys. Rev. Lett.* **100**, 236101 (2008).
- [10] B. Pettinger, P. Schambach, C. J. Villagómez, and N. Scott, *Annu. Rev. Phys. Chem.* **63**, 379 (2012).
- [11] B. Pettinger, G. Picardi, R. Schuster, and G. Ertl, *Single Mol.* **3**, 285 (2002).
- [12] A. Dazzi, R. Prazeres, F. Glotin, and J. M. Ortega, *Opt. Lett.* **30**, 2388 (2005).
- [13] A. Dazzi, C. B. Prater, Q. Hu, D. B. Chase, J. F. Rabolt, and C. Marcott, *Appl. Spectrosc.* **66**, 1365 (2012).
- [14] J. R. Felts, K. Kjoller, M. Lo, C. B. Prater, and W. P. King, *ACS Nano* **6**, 8015 (2012).
- [15] B. Lahiri, G. Holland, and A. Centrone, *Small* **9**, 439 (2013).
- [16] V. Krishna and J. C. Tully, *J. Chem. Phys.* **125**, 054706 (2006).
- [17] Y. Wang, E. Kioupakis, X. Lu, D. Wegner, R. Yamachika, J. E. Dahl, R. M. K. Carlson, S. G. Louie, and M. F. Crommie, *Nat. Mater.* **7**, 38 (2008).
- [18] J. E. Dahl, S. G. Liu, and R. M. K. Carlson, *Science* **299**, 96 (2003).
- [19] X. Hong, X. Shen, M. Gong, and F. Wang, *Opt. Lett.* **37**, 4982 (2012).
- [20] M. Völcker, W. Krieger, T. Suzuki, and H. Walther, *J. Vac. Sci. Technol. B* **9**, 541 (1991).
- [21] T. Holstein, *Phys. Rev.* **88**, 1427 (1952).
- [22] M. M. Fulk and M. M. Reynolds, *J. Appl. Phys.* **28**, 1464 (1957).
- [23] L. J. Lauhon and W. Ho, *Rev. Sci. Instrum.* **72**, 216 (2001).
- [24] A. Troisi and M. A. Ratner, *J. Chem. Phys.* **125**, 214709 (2006).
- [25] J. B. Maddox, U. Harbola, N. Liu, C. Silien, W. Ho, G. C. Bazan, and S. Mukamel, *J. Phys. Chem. A* **110**, 6329 (2006).
- [26] J. Oomens, N. Polfer, O. Pirali, Y. Ueno, R. Maboudian, P. W. May, J. Filik, J. E. Dahl, S. Liu, and R. M. K. Carlson, *J. Mol. Spectrosc.* **238**, 158 (2006).
- [27] F. M. Hoffmann, *Surf. Sci. Rep.* **3**, 107 (1983).
- [28] P. R. Schreiner, L. V. Chernish, P. A. Gunchenko, E. Yu. Tikhonchuk, H. Hausmann, M. Serafin, S. Schlecht, J. E. P. Dahl, R. M. K. Carlson, and A. A. Fokin, *Nature (London)* **477**, 308 (2011).
- [29] A. A. Fokin, L. V. Chernish, P. A. Gunchenko, E. Yu. Tikhonchuk, H. Hausmann, M. Serafin, J. E. P. Dahl, R. M. K. Carlson, and P. R. Schreiner, *J. Am. Chem. Soc.* **134**, 13 641 (2012).